Available online at www.sciencedirect.com

SCIENCE DIRECT®

Journal of Solid State Chemistry 177 (2004) 3038–3044

JOURNAL OF SOLID STATE CHEMISTRY

http://elsevier.com/locate/jssc

Building three-dimensional metal phosphites from the corner-shared four-membered rings chain

Shi Suhua, Qian Wei, Li Guanghua, Wang Li, Yuan Hongming, Xu Jianing,
Zhu Guangshan, Song Tianyou,* and Qiu Shilun*

Department of Chemistry, The State Key Laboratory of Inorganic Synthesis and Preparative Chemistry, Jilin University, Changchun 130023, China

Received 1 March 2004; received in revised form 29 April 2004; accepted 2 May 2004

Abstract

Three new compounds, a one-dimensional (1D) zinc phosphite, $(C_4H_8N_2H_4)[Zn(HPO_3)_2]$ (**I**), two three-dimensional (3D) metal phosphites $(C_4H_8N_2H_4)[Zn_3(HPO_3)_4]$ (**II**) and $(C_4H_8N_2H_4)[Zn_{(3-x)}Co_x(HPO_3)_4(H_2O)_2]$ ($x \approx 0.83$) (**III**) have been synthesized under hydrothermal conditions templated by piperazine and characterized by single-crystal X-ray diffraction, XRD, IR, UV-vis spectra and SQUID magnetometer. Compound **I** displays 1D chain-like structure, containing corner-shared (cs) four-membered rings. Interestingly, the structures of **II** and **III** show 1D chains similar to those observed in **I**. It is noteworthy that **III** represents the first cobalt-substituted zinc-phosphite. Crystal data: **I**, monoclinic, $C2/c$, $a = 17.748(2)$ Å, $b = 7.428(9)$ Å, $c = 8.8071(11)$ Å, $\beta = 105.345(3)^\circ$, $V = 1091.9$ Å^3, $Z = 4$. **II**, Monoclinic $P2_1/c$, $a = 9.9435(4)$ Å, $b = 10.1438(3)$ Å, $c = 17.8164(5)$ Å, $\beta = 95.665(2)^\circ$, $V = 1788.27$ Å^3, $Z = 4$, and **III**, Monoclinic $P2_1/c$, $a = 7.2338(2)$ Å, $b = 15.0238(5)$ Å, $c = 9.2153(3)$ Å, $\beta = 107.741(2)^\circ$, $V = 953.88(5)$ Å^3, $Z = 2$.

Keywords: Hydrothermal synthesis; Metal phosphites; Piperazine; Pseudo-pyramids; Magnetic properties

1. Introduction

In recent years, a variety of metal phosphates with open-framework have been prepared and characterized [1]. Open-framework materials are of great interests from both the industrial and academic points of view because of their applications in the field of catalysis, adsorption, ion exchange, etc. Currently, interests in transition metal open-framework have been focused on metal phosphites of zeolite-type structure. Unlike phosphates, the first row transition metal phosphites have been rarely studied. Only a few organically templated V(IV) [2,3], V(III) [4], Cr(III) [5], Mn(II) [6,7], Fe(III) [4], Co(II) [8], Zn(II) [9–16] phosphites have been synthesized and characterized recently. In the family of open-framework metal phosphites, zinc phosphites hold an important position and those with three-dimensional (3D) open-framework [9–15]; two-dimensional (2D) layers structure [10,16]; one-dimensional (1D) polymeric chain and small molecule [10] have been prepared and characterized. However, transition-metal-substituted zincphosphites have never been reported. To our knowledge, only a few of transition-metal-doped zincophosphates have been characterized [17–19]. Partial substitution of the zinc atoms in the framework by divalent cobalt atom may result in interesting magnetic properties and the potential catalytic performance, which prompts us to investigate the cobalt-containing zincphosphites. Herein, we report three new zinc-phosphites $(C_4H_8N_2H_4)[Zn(HPO_3)_2]$ (**I**), $(C_4H_8N_2H_4)[Zn_3(HPO_3)_4]$ (**II**), and $(C_4H_8N_2H_4)[Zn_{(3-x)}Co_x(HPO_3)_4(H_2O)_2]$ (**III**), which are synthesized under hydrothermal conditions in the presence of piperazine. The structure of all the three compounds contain the complete 1D chains formed by the corner-shared (cs) four-membered rings. Moreover, compound **III** is the first example of zinc-phosphite partially substituted by cobalt(II) templated by piperazine.

---

*Corresponding authors. Fax: +86-431-5671974.

E-mail address: lhl222@mail.jlu.edu.cn (Q. Shilun).

0022-4596/$ - see front matter © 2004 Elsevier Inc. All rights reserved.
doi:10.1016/j.jssc.2004.05.002

2. Experimental section

2.1. Syntheses and initial characterization

Synthesis of $(C_4H_8N_2H_4)[Zn(HPO_3)_2]$ (**I**): In a typical synthesis, single crystals of **I** were obtained by mixing $ZnAc_2 \cdot 2H_2O$ (0.549 g), H_3PO_3 (1.025 g), piperazine hexahydrate (2.425 g), $H_2C_2O_4 \cdot 2H_2O$ (0.630 g) and water (9 mL) in a molar ratio of $ZnAc_2$:H_3PO_3:piperazine:$H_2C_2O_4$:$H_2O = 1:5:5:1:200$. The mixture was subsequently heated at 393 K for 4 days in a Teflon autoclave under the autogenous pressure (filling degree: ~60%; pH: ~6) and followed by slow cooling down to room temperature. The resulting rod-like crystals were washed with distilled water and dried in air.

Synthesis of $(C_4H_8N_2H_4)[Zn_3(HPO_3)_4]$ (**II**): $ZnAc_2 \cdot 2H_2O$ (1.098 g), H_3PO_3 (1.230 g), piperazine hexahydrate (1.940 g), $H_2C_2O_4 \cdot 2H_2O$ (0.630 g) and water (9 mL) were mixed in a molar ratio of $ZnAc_2$: H_3PO_3:piperazine:$H_2C_2O_4$:$H_2O = 1:1:2:1:200$. The mixture was subsequently heated at 423 K for 3 days in a Teflon autoclave under the autogenously pressure (filling degree: ~55%; pH: ~5), and followed by slow cooling down to room temperature. The resulting crystals were washed with distilled water and dried in air.

Synthesis of $(C_4H_8N_2H_4)[Zn_{(3-x)}Co_x(HPO_3)_4(H_2O)_2]$ (**III**): $ZnAc_2 \cdot 2H_2O$ (0.552 g), $CoCl_2 \cdot 6H_2O$ (0.199 g), H_3PO_3 (0.546 g), piperazine hexahydrate (1.295 g) and water (10 mL) were mixed in a molar ratio of $CoCl_2$:$ZnAc_2$:H_3PO_3:piperazine:$H_2O = 1:3:8:8:200$. The mixture was subsequently heated at 423 K for 3 days in a Teflon autoclave under the autogenous pressure (filling degree: ~55%; pH: ~5), and followed by slow cooling down to room temperature. The resulting crystals were washed with distilled water and dried in air.

2.2. Characterizations

The initial characterization was carried out using powder X-ray diffraction (XRD), inductively coupled plasma (ICP) and elemental analysis, and infrared spectroscopy (IR) for **I**–**III**. Only the diffuse-reflectance UV-vis spectroscopy and magnetic susceptibility was measured for **III**.

Powder XRD patterns for the structure of **I**–**III** indicated that the structures of the compounds were novel, and the patterns were entirely consistent with the simulated one on the basis of the single-crystal diffraction. The ratio of zinc: phosphorus was determined by ICP atomic emission spectroscopy (ICP-AES). Elemental analyses were performed on a Perkin-Elmer 240C element analyzer, indicating a Zn:P of 1:2 for **I**, 3:4 for **II**, and (Zn + Co):P of 0.36:0.49 (The Zn:Co molar ratio is 0.282:0.078) for **III**. They are in good agreement with the values obtained from the single-crystal XRD analysis. Elemental analysis results of compounds **I**–**III** are also consistent with the stoichiometry. Anal. Calcd. for **I**: C, 15.31; H, 4.46; N, 8.93; Found: C, 15.28; H, 4.49; N, 9.00. Calcd. for **II**: C, 7.94; H, 2.65; N, 4.63; Found: C, 7.90; H, 2.71; N, 4.49. Calcd. for **III**: C, 7.50; H, 3.12; N, 4.37; Found: C, 7.55; H, 3.39; N, 4.42.

Thermogravimetric analysis (TGA) of **I**–**III** were carried out on a Perkin-Elmer TGA 7 thermogravimetric analyzer, with a heating rate of $10^\circ C\,min^{-1}$ under static nitrogen from room temperature to 800°C. Compound **I** displayed a mass loss of 27.25 wt% at 250–450°C, consistent with the loss of the organic template (theoretical loss 28.07 wt%). In the case of **II**, the mass at 366°C followed by a tail of 11.9 wt% in the 420–800°C range corresponds to the loss of the amine. In the case of **III**, It shows an obvious weight loss of 13.46 wt% at 180–270°C, consistent with the loss of piperazine (theoretical loss 13.87 wt%) in the product and weight loss of 10.65 wt% at 345–385°C is attributed to the loss of H_2O (11.34 wt%) in the framework. XRD analysis indicated that the compounds became non-crystalline after the decomposition of the occluded template.

Infrared (IR) spectra of **I**–**III** were recorded in the range 400–4000 cm^{-1} using the KBr pellet method. The IR spectra of all three compounds showed typical peaks, which confirmed that piperazinium cation (ν_{N-H}, ν_{C-C}, ν_{C-N}, 2500–3240, 1450–1630 cm^{-1}), water molecular (ν_{O-H}, 3363 cm^{-1}), P–H bonds (ν_{P-H}, 2373, 2381, 2360 cm^{-1}) and P–O bonds (ν_{P-O}, 990–1180 and 460–600 cm^{-1}) were in presence [20,21].

UV-vis spectra: Diffuse reflectance spectra of **III** in the visible range (VARIAN Cary 500) were collected on a Shimadzu UV-365 spectrometer within the range of 300–800 nm. The spectra of $(C_4H_8N_2H_4)[Zn_{(3-x)}Co_x(HPO_3)_4(H_2O)_2]$, $(C_2H_{10}N_2)_{0.5}[CoPO_4]$ (DAF-2) [22] and $NH_4[(Zn_{1-x}Co_x)BP_2O_8]$ ($0 \leqslant x \leqslant 0.14$) [23] ($Co^{2+}$ in tetrahedral coordination) were also recorded for comparison purpose.

The magnetization of compound **III** was measured on Quanfum Design SQUID XL-5 in a field of 1000 Oe. Magnetic susceptibility dependence of temperature curve was obtained in the range 300–2 K.

XRD analysis: three crystals with dimensions of 0.21 × 0.17 × 0.17 nm for **I**, 0.80 × 0.35 × 0.35 nm for **II** and 0.35 × 0.35 × 0.30 nm for **III** were selected for indexing and mounted on a thin glass fiber with cyanoacrylate adhesive. The intensity data were collected on a Siemens Smart CCD diffractometer. No significant decay was observed during the data collection. Data were processed on a Pentium PC using Bruker Axs Windows NT SHELXTL software package (version 5.10) [24,25]. Neutral atom scattering factors were taken from Cromer and Waber [26]. Empirical absorption correction was applied. All structures were solved by the direct method. One of phosphorus atoms

[P(2)] of the anion framework in **II** was found to be disordered. The positions of hydrogen atoms were either located or calculated and their contributions in structural factor calculations were included. The crystallographic data of **I–III** are summarized in Table 1, selected bond lengths/angles data are presented in Table 2.

3. Results and discussion

3.1. Description of the crystal structure

Crystal Structure of $(C_4H_8N_2H_4)[Zn(HPO_3)_2]$, (**I**): The asymmetric unit of **I** consists of 8 non-hydrogen atoms (1Zn, 1P, 3O, 1N and 2C). Each zinc center

Table 1
Crystal data and structure refinement for **I–III**

Empirical formula	$C_4H_{14}N_2O_6P_2Zn$	$C_4H_{16}N_2O_{12}P_4Zn_3$	$C_4H_{20}N_2O_{14}P_4Zn_{(3-x)}Co_x$
Formula weight	313.48	604.18	634.69
Temperature (K)	293(2)	293(2)	293(2)
Crystal system, space group	Monoclinic, $C2/c$	Monoclinic, $P2_1/c$	Monoclinic, $P2_1/c$
a (Å)	17.748(2)	9.9435(4)	7.2338(2)
b (Å)	7.2428(9)	10.1438(3)	15.0238(5)
c (Å)	8.8087(11)	17.8164(5)	9.2153(3)
β (deg)	105.345(3)	95.665(2)	107.741(2)
Volume (Å^3)	1091.9(2)	1788.27(10)	953.88(5)
Z, Calculated density (Mg/m^3)	4, 1.907	4, 2.244	2, 2.229
Reflections collected/unique	2043/778 [$R_{int} = 0.0355$]	8091/2556 [$R_{int} = 0.0469$]	4478/1365 [$R_{int} = 0.0406$]
Max. and min. transmission	0.3509 and 0.2809	0.3341 and 0.1873	0.4169 and 0.2684
Data/restraints/parameters	778/0/73	2556/0/247	1365/0/140
Goodness-of-fit on F^2	1.101	1.019	1.083
Final R indices [$I > 2\sigma(I)$]	$R_1 = 0.0229$, w$R_2 = 0.0588$	$R_1 = 0.0257$, w$R_2 = 0.0678$	$R_1 = 0.0290$, w$R_2 = 0.0829$
R indices (all data)	$R_1 = 0.0258$, w$R_2 = 0.0609$	$R_1 = 0.0319$, w$R_2 = 0.0702$	$R_1 = 0.0334$, w$R_2 = 0.0848$
Largest diff. peak and hole (e Å^{-3})	0.331 and −0.303	0.469 and −0.390	0.424 and −1.073

Table 2
Selected bond lengths (Å) and angles (deg) for **I–III**

$(C_4H_8N_2H_4)[Zn(HPO_3)_2]$					
Zn(1)–O(2)	1.923(2)	P(1)–O(2)[a]	1.510(2)	P(1)–O(1)–Zn(1)	137.95(14)
Zn(1)–O(1)	1.941(2)	P(1)–O(1)	1.515(2)	P(1)[a]–O(2)–Zn(1)	133.15(13)
P(1)–O(3)	1.510(2)	P(1)–H(1)	1.30 (2)		
$(C_4H_8N_2H_4)[Zn_3(HPO_3)_4]$					
Zn(1)–O(4)	1.911(3)	P(1)–O(1)	1.514(3)	P(4)–H(4)	1.34(4)
Zn(1)–O(2)	1.921(2)	P(1)–O(9)	1.522(3)	P(4)–O(10)–Zn(3)	128.59(15)
Zn(1)–O(1)	1.930(3)	P(1)–H(1)	1.27(4)	P(1)–O(1)–Zn(1)	124.12(16)
Zn(1)–O(3)	1.960(2)	P(2)–O(11)[b]	1.382(4)	P(2)–O(2)–Zn(1)	117.14(18)
Zn(2)–O(5)	1.922(3)	P(2)–O(6)	1.558(3)	P(3)–O(3)–Zn(1)	126.83(15)
Zn(2)–O(8)	1.930(3)	P(2)–O(2)	1.597(3)	P(4)[f]–O(4)–Zn(1)	137.55(18)
Zn(2)–O(6)	1.937(3)	P(3)–O(12)[c]	1.496(3)	P(1)–O(5)–Zn(2)	140.81(18)
Zn(2)–O(7)	1.953(3)	P(3)–O(7)[d]	1.506(3)	P(2)[h]–O(11)–Zn(3)	144.7(3)
Zn(3)–O(11)	1.904(3)	P(3)–O(3)	1.523(3)	P(2)–O(6)–Zn(2)	127.12(19)
Zn(3)–O(12)	1.910(3)	P(3)–H(3)	1.35(3)	P(3)[g]–O(7)–Zn(2)	129.89(16)
Zn(3)–O(10)	1.939(2)	P(4)–O(8)[e]	1.497(3)	P(4)[e]–O(8)–Zn(2)	140.1(2)
Zn(3)–O(9)	1.953(3)	P(4)–O(4)[c]	1.501(3)	P(1)–O(9)–Zn(3)	121.84(16)
P(1)–O(5)	1.509(3)	P(4)–O(10)	1.517(3)	P(3)[f]–O(12)–Zn(3)	143.42(17)
$(C_4H_8N_2H_4)[Zn_{(3-x)}Co_x(HPO_3)_4(H_2O)_2]$					
Zn(1)–O(1)	1.912(3)	P(1)–O(1)	1.514(4)	P(2)–H(2)	1.40(4)
Zn(1)–O(3)	1.930(3)	P(1)–O(5)	1.516(3)	P(1)–O(5)–Zn(2)	127.85(18)
Zn(1)–O(2)	1.945(3)	P(1)–O(3)[i]	1.533(3)	P(2)[l]–O(6)–Zn(2)	137.71(19)
Zn(1)–O(4)	1.945(3)	P(1)–H(1)	1.27(4)	P(1)–O(1)–Zn(1)	138.7(2)
Zn(2)–O(6) × 2	2.068(3)	P(2)–O(6)[j]	1.498(3)	P(2)–O(2)–Zn(1)	131.7(2)
Zn(2)–O(5) × 2	2.105(3)	P(2)–O(2)	1.531(3)	P(1)[k]–O(3)–Zn(1)	137.8(2)
Zn(2)–O(7) × 2	2.142(4)	P(2)–O(4)[k]	1.532(3)	P(2)[i]–O(4)–Zn(1)	130.7(2)

Symmetry transformations used to generate equivalent atoms: [a] $-x, -y, -z+2$, [b] $x-1, y, z$, [c] $-x+2, y-1/2, -z+3/2$, [d] $x, -y+1/2, z+1/2$, [e] $-x+2, -y, -z+1$, [f] $-x+2, y+1/2, -z+3/2$, [g] $x, -y+1/2, z-1/2$, [h] $x+1, y, z$, [i] $x, -y+1/2, z-1/2$, [j] $x+1, y, z+1$, [k] $x, -y+1/2, z+1/2$, [l] $x-1, y, z-1$.

adopts typical tetrahedral coordination geometry with four oxygen atoms occupying each coordination site. The average Zn–O bond length is 1.932(2) Å, which is close to the value reported [12]. Each HPO_3 unit adopts pseudo-pyramid geometry with three oxygen atoms (two bridging oxygen atoms and one terminal oxygen atom O3) and a hydrogen atom on the four vertices and a phosphorus atom in the center. The P–H bond length of compound **I** is 1.30(2) Å and is similar to the previously reported P–H bond length in H_3PO_3 [27]. The presence of P–H bonds has also been confirmed by the characteristic IR signal (ν_{H-P} 2373 cm^{-1}) for P–H stretch in phosphite anions [20,27]. Two Zn(1) atoms and two P(1) atoms can form a cs four-membered ring by linkage of oxygen bridges, resulting in an infinite chain structure (Fig. 1 below). The framework structure consists of the chains and the diprotonated piperazines via hydrogen bonding interactions between the terminal oxygens (O3) in these chains and the nitrogen atoms of piperazines (Fig. 1 top).

Crystal structure of $(C_4H_8N_2H_4)[Zn_3(HPO_3)_4]$, (**II**): Compound **II** displays a 3D network structure, involving ZnO_4 tetrahedra and HPO_3 pseudo-pyramid. The asymmetric unit of **II** consists of 25 non-hydrogen atoms, of which nineteen belong to the framework and six belong to the guest species. There are three crystallographically independent zinc and four phosphorus atoms. All Zn atoms are linked to the P atoms via oxygen bridges. The Zn–O bond lengths are in the range of 1.904(3)–1.960(2) Å (av. 1.931 Å) and the O–Zn–O angles are in the range of 96.85(13)–116.38(12)° (av. 109.4°), which are typical for Zn atoms in a tetrahedral environment. All HPO_3 units adopt pseudo-pyramidal geometry, with the average P–O bond length of ~1.506 Å and the average P–H bond length of ~1.32 Å (the characteristic IR signal ν_{H-P} 2381 cm^{-1}). Zn(1), Zn(2), P(1), P(2), P(3) and P(4) are linked through oxygen bridges, leading to the formation of infinite cs four-remembered ring chains (Fig. 2 below). There are two different types of four-membered rings within each chain (one containing Zn(1), Zn(2), P(1) and P(2); the other containing Zn(1), Zn(2), P(3) and P(4)). The linear chains are similar to those found in compound **I**, which are further cross-linked together by $Zn(3)O_4$ tetrahedra to generate eight-membered channels (Fig. 2 top) along the (001) directions, where the diprotonated piperazine cations reside.

Crystal structure of $(C_4H_8N_2H_4)[Zn_{(3-x)}Co_x(HPO_3)_4(H_2O)_2]$, (**III**): The UV-vis diffuse-reflectance spectrum of compound **III** exhibits three absorption maxima at 546, 586, and 631 nm (Fig. 3), close to those for the previously discovered CoPO-GIS (a novel 3D

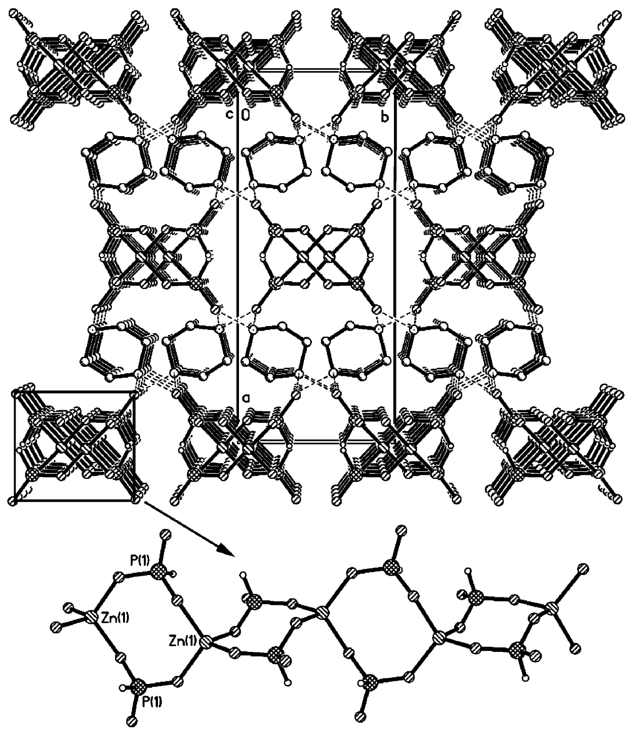

Fig. 1. (Top) The structure of $(C_4H_{12}N_2)[Zn(HPO_3)_2]$, dotted lines represent hydrogen bond interactions between the amine molecules and framework oxygens. (Below) A fragment of a cs four-ring chain in $[Zn(HPO_3)_2]^{2-}$ structure.

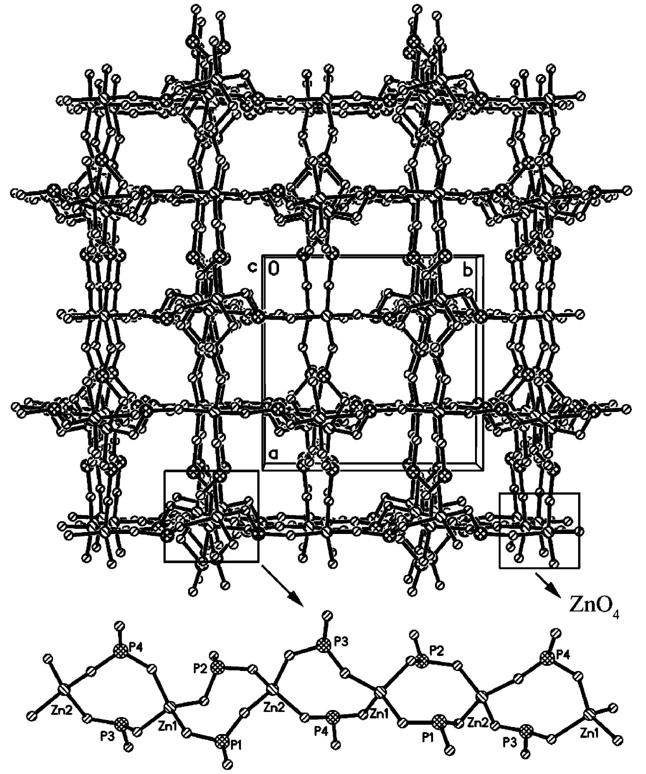

Fig. 2. (Top) View of the structure of $[Zn_3(HPO_3)_4]^{2-}$ (along the *c*-axis). (Below) showing cs four-rings chain structure derived from compound **II** (H atoms omitted for clarity).

network cobalt phosphate with a composition of $[(NH_3CH_2CH_2NH_3)_{0.5}CoPO_4]$ containing tetrahedral CoO_4 units [28]). These absorption maxima can be attributed to the $d-d$ transitions of tetrahedrally coordinated Co^{2+} with a d^7 configuration [29]. It could be concluded that the Co(II) ions are tetrahedrally coordinated in the crystal lattice, which is also consistent with the blue color of the compound. Similar cobalt-doping zincophosphates have been reported previously in open-framework zinc phosphate materials [18,19].

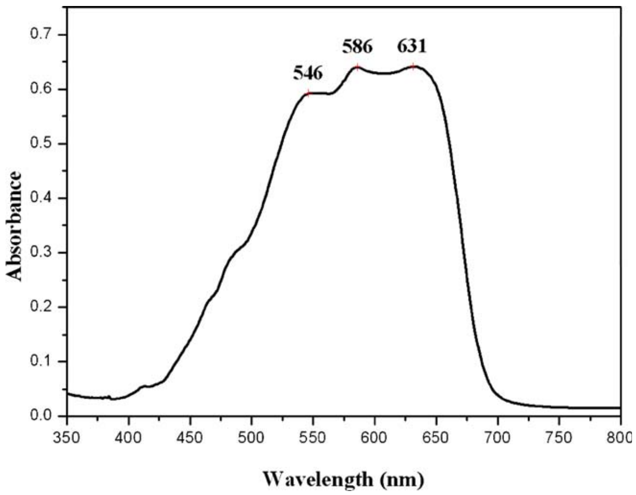

Fig. 3. Diffuse reflectance spectra of compound **III**.

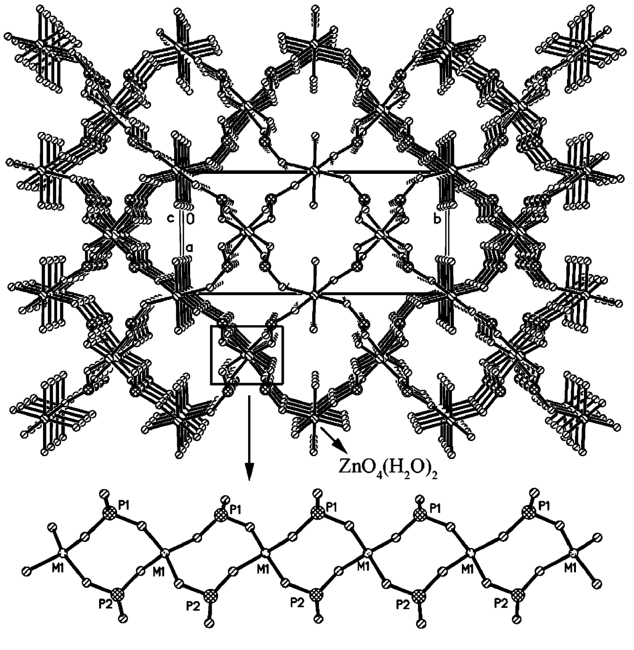

Fig. 4. (Top) View of the structure of $[Zn_{3-x}Co_x(HPO_3)_4(H_2O)_2]^{2-}$, along the *c*-axis (Below) showing cs four-rings chain structure derived from **III**. H atoms are not shown.

The compound **III** is a blue crystal with a high degree of cobalt-substitution on the zinc site. And Co:Zn ratio of 1:3.6 was found in the ICP analysis, corresponding to the composition $Co_{0.83}Zn_{2.17}$. The asymmetric unit of **III** consists of 14 non-hydrogen atoms, of which eleven belong to the framework and three belong to the guest species. Of the two unique metal atoms, $M(1)$ (Zn(1) or Co) is tetrahedrally coordinated by four oxygen atoms with the average bond length and bond angle of 1.933 Å and 109.5°, respectively, while $M(2)$ ($M(2) = Zn(2)$) is octahedrally coordinated by four oxygen atoms of phosphite ($M(2)$–$O_{av.}$ 2.087 Å) and two oxygen atoms of water molecules in a *trans* fashion (the average $M(2)$–O_{water} bond length is 2.142 Å) [30,31]. All HPO_3 units possess a pseudo-pyramidal geometry, with the average P–O and P–H bond lengths of ~1.521 and ~1.335 Å, respectively (the characteristic IR signal ν_{H-P} 2360 cm^{-1}).

The strictly alternating $M(1)O_4$ and $HP(1)O_3$ or $HP(2)O_3$ tetrahedral units form four-membered rings, which are linked through their corners forming 1D chains (Fig. 4 below). The individual chain units are further linked together by the bridging oxygen of the $Zn(2)O_4(H_2O)_2$ octahedra connecting to the oxygen of the phosphite of the linear chains to form the 3D architecture with 2D intersecting eight-membered ring channels. It is interesting to note that there are two different types of eight-membered ring channels along [001] directions (Fig. 4 top) (type A: the terminal water molecules that coordinate to the Zn centers stick out into the channels, which causes the partial blockage of the channels; type B: the Zn atoms are only coordinated by oxygen atoms of phosphites and the phosphites P–H bonds project into the channels, leading to partial blockage of the channels). The piperazine dictation templates are located in the clear channels along [100] direction, Hydrogen bonds are found between the piperazine nitrogen atoms and the oxygen atoms of the framework (Fig. 5).

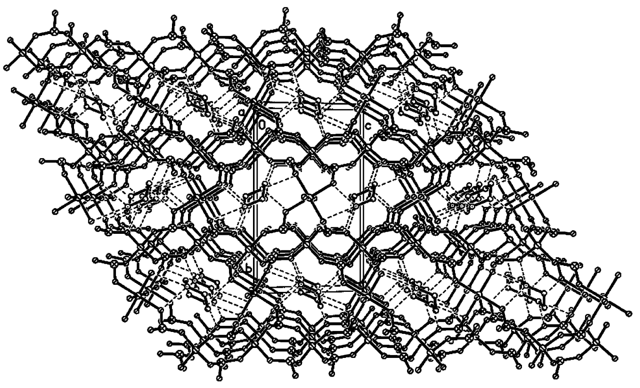

Fig. 5. View along the *a*-axis showing cs four-rings chain and P-based polyhedra linked by $ZnO_4(H_2O)_2$ octahedra.

4. Discussion

Three new zincophosphites with the same organically templated, $(C_4N_2H_{12})[Zn(HPO_3)_2]$ (**I**), $(C_4N_2H_{12})[Zn_3(HPO_3)_4]$ (**II**) and $(C_4N_2H_{12})[Zn_{(3-x)}Co_x(HPO_3)_4(H_2O)_2]$ (**III**), have been prepared as single crystals by the hydrothermal conditions and structurally characterized by X-ray methods. Although the dimensionalities of the frameworks $(C_4N_2H_{12})[Zn(HPO_3)_2]$ (1D), $(C_4N_2H_{12})[Zn_3(HPO_3)_4]$ (3D) and $(C_4N_2H_{12})[Zn_{(3-x)}Co_x(HPO_3)_4(H_2O)_2]$ (3D), their structures are quite closely related, they consist of the linear cs four-ring chains that are built from the typical polyhedral unit of MO_4 tetrahedral and HPO_3 pseudo-pyramid units, sharing vertices [12]. Similar cs four-ring chains have been observed previously in aluminum phosphate $[AlP_2O_8H_x]^{3-x}$ ($x = 1, 2$) [32] and zinc phosphate $[Zn(HPO_4)_2]^{2-}$ [33], and considered to be the primary building block (or so called parent chain) in one model proposed for the formation of phosphates possessing open structures [32]. The formation of 1D, 2D and 3D structure based on the cs four-ring chain may be rationalized using the parent chain model and therefore, the isolation of cs four-ring zinc phosphite chain architectures will be important. The transformations of low-dimensional zinc phosphites to complex open-framework structures are currently being investigated in our laboratory. In addition, $(C_4N_2H_{12})[Zn_3(HPO_3)_4]$ (**II**) and $(C_4N_2H_{12})[Zn_{(3-x)}Co_x(HPO_3)_4(H_2O)_2]$ (**III**) are closely related to $(C_4N_2H_{12})_{0.5}[Zn(HPO_4)(H_2PO_4)]$ [34], with all three phases showing the same piperazinium template cation, and cs four-ring ZnPO chain architecture. A notable difference between the three 3D open-frameworks is originated from the diverse link of cs four-ring chains. The structure of $(C_4N_2H_{12})_{0.5}[Zn(HPO_4)(H_2PO_4)]$ is based on a network connected by infinite ZnPO chains in different directions that involve ZnO_4, $PO_3(OH)$ and $PO_2(OH)_2$ tetrahedra, whereas in II and III, the connection between the ZnO_4 (or $ZnO_4(H_2O)_2$) units and the bridging oxygens of the HPO_3 in the neighboring four chains give rise to new topologies.

In order to balance the charge of the anionic framework, the piperazine molecules are fully protonated in **I–III**. Each NH_2 group forms two hydrogen bonds with the oxygen atoms of the framework. The multiple hydrogen bonds play a key role in the formation and the stability of the open architectures. In **I–III**, the piperazine dictations interact with the framework through strong hydrogen bonds, as evidenced by the short $N\cdots O$ distances ($\sim$2.7–3.0 Å) and the $N–H\cdots O$ angles of $>160°$. The important hydrogen bonding interactions are listed in Table 3.

Table 3
Hydrogen bonds lengths (Å) and angles (deg) for **I–III**

$D–H\cdots A$	$d(D–H)$	$d(H\cdots A)$	$d(D\cdots A)$	$<(DHA)$
$(C_4H_8N_2H_4)[Zn(HPO_3)_2]$				
$N(1)–H(1A)\cdots O(3)^a$	0.90	1.82	2.711(3)	170.1
$N(1)–H(1B)\cdots O(3)$	0.90	1.80	2.675(3)	111.8
$(C_4H_8N_2H_4)[Zn_3(HPO_3)_4]$				
$N(1)–H(1A)\cdots O(9)$	0.90	1.90	2.789(4)	168.6
$N(1)–H(1B)\cdots O(6)^b$	0.90	2.03	2.931(4)	177.9
$N(2)–H(2A)\cdots O(3)^c$	0.90	1.87	2.770(4)	177.8
$N(2)–H(2B)\cdots O(10)^c$	0.90	2.00	2.874(4)	164.5
$(C_4H_8N_2H_4)[Zn_{(3-x)}Co_x(HPO_3)_4(H_2O)_2]$				
$O(7)–H(7A)\cdots O(4)^d$	0.72(5)	2.10(5)	2.806(6)	165(5)
$O(7)–H(7B)\cdots O(3)^e$	0.64(5)	2.22(5)	2.847(6)	167(6)
$N(1)–H(1A)\cdots O(2)^f$	0.90	1.91	2.787(5)	164.9
$N(1)–H(1B)\cdots O(5)$	0.90	1.81	2.704(5)	175.2

Symmetry transformations used to generate equivalent atoms: $^a x, -y-1, z+1/2$, $^b x+1, y, z$, $^c x, -y+1/2, z-1/2$, $^d -x+1, y+1/2, -z-1/2$, $^e x, -y+1/2, z-1/2$, $^f -x+1, -y+1, -z$.

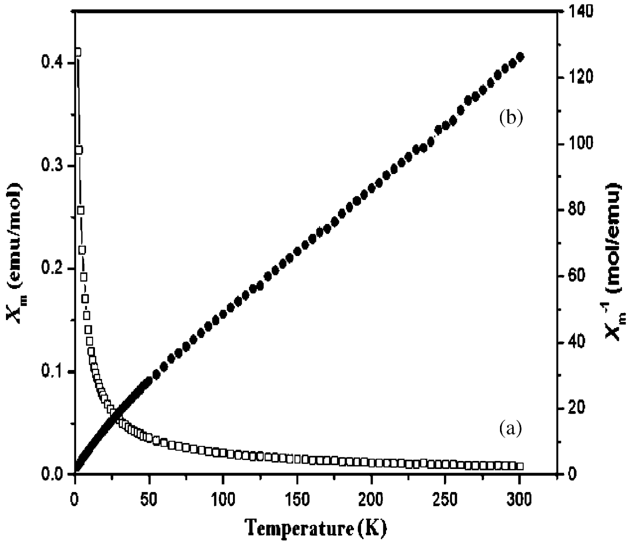

Fig. 6. Thermal evolution of X_m (a) and X_m^{-1} (b) curves of **III**.

The syntheses of **I** and **II** have been carried out by the addition of oxalic acid in addition to H_3PO_3. No $C_2O_4^{2-}$ ions were found in these structures though we expected that oxalic acid would work as a ligand to form oxalate-phosphite frameworks. Contrast to the above-mentioned recipes, **I** and **II** cannot be obtained in the reaction systems without adding oxalic acids, so it may act as a mineralizer similar to the F^- ions in certain syntheses of the phosphates of Al and Ga [35], as earlier studies within the family of zinc phosphates have indicated an improvement in the crystallinity of the products [36].

The magnetic measurements of **III** were carried out on powdered sample from 300 to 2 K. Both X_m and X_m^{-1} vs. T curves are shown in Fig. 6. Between 300 and 45 K, the $1/X_m = f(T)$ curve obeys a Curie–Weiss law $X_m = C/(T-\theta)$, where $C = 2.598\,\mathrm{emu\,K\,mol^{-1}}$ and

$\theta = -25.32\,\mathrm{K}$. This Weiss constant is indicative of antiferromagnetic exchange interactions between the Co(II) cations in **III**. In order to calculate the magnetic moments of the Co(II) ions, we assumed that the diamagnetic Zn(II) ions does not contribute significantly to the total magnetic moment of **III**. The effective magnetic moment calculated from the formula $\mu_{\text{eff}} = \sqrt{8\chi_{\text{m}}T}$ at 300 K is 5.24 μ_{B} per Co atom, which is somewhat higher than the spin-only value (3.87 μ_{B}) for Co(II) but is close to experimentally observed moments for tetrahedral Co(II) complexes [37] and layered cobalt phosphates reported by Zubieta et al. [38].

5. Conclusion

In conclusion, three new zinc (zinc–cobalt) phosphites have been synthesized under hydrothermal conditions using piperazine as a structure directing agent and their structures have been successfully characterized by single XRD methods. Interestingly, of the structure of these compounds, 3D metal phosphites are built up from linear cs four-membered rings chain that consists of MO_4 (M=Zn or Co) tetrahedra and HPO_3 pseudo-pyramids. It is noteworthy that the compound III is the first organically templated zinc-cobalt phosphite. Since the analogous structure of this zinc-cobalt phosphite has not been found in zinc or cobalt phosphites, the synthesis of this 3D phosphite is important. Our results show that it is possible to use mixed metals to synthesize new open framework phosphite structures.

CCDC reference number 212270-212272. Copies of this data can be obtained free of charge on application to CCDC, 12 Union Road, Cambridge CB2 1EZ, UK (fax: +44-1223-336-033; mail to: deposit@ccdc.cam.ac.uk or www: http://www.ccdc.cam.ac.uk).

Acknowledgments

This work was supported by the State Basic Research Project (G2000077507), and the National Science Foundation of China (No. 29873017 and 20101004). We thank Hong Ding for ICP analysis and Lianxiang Yu for IR analysis.

References

[1] A.K. Cheetham, T. Loisseau, G. Ferey, Angew. Chem. Int. Ed. 38 (1999) 3268.

[2] W.T.A. Harrison, Solid State Sci. 18 (2002) 1.

[3] G. Bonavia, J.R.D. DeBord, R.C. Haushalter, D. Rose, J. Zubieta, J. Chem. Mater. 7 (1995) 1995.

[4] S. Fernández, J.L. Pizarro, L. Lezama, M.I. Arriortua, T. Rojo, Chem. Mater. 14 (2002) 2300.

[5] S. Fernández, J.L. Mesa, J.L. Pizarro, L. Lezama, M.I. Arriortua, T. Rojo, Angew. Chem. Int. Ed. 41 (2002) 3683.

[6] S. Fernández, J.L. Mesa, J.L. Pizarro, L. Lezama, M.I. Arriortua, R. Olazcuaga, T. Rojo, Chem. Mater. 12 (2000) 2092.

[7] S. Fernández, J.L. Pizarro, J.L. Mesa, L. Lezama, M.I. Arriortua, R. Olazcuaga, T. Rojo, Inorg. Chem. 40 (2001) 3476.

[8] S. Fernández, J.L. Pizarro, J.L. Mesa, L. Lezama, M.I. Arriortua, T. Rojo, Int. J. Inorg. Mater. 3 (2001) 331.

[9] W.T.A. Harrison, J. Solid State Chem. 160 (2001) 4.

[10] W.T.A. Harrison, M.L. Phillips, T.M. Nenoff, Int. J. Inorg. Mater. 3 (2001) 1033.

[11] J.A. Rodgers, W.T.A. Harrison, Chem. Commun. (2000) 2385.

[12] W.T.A. Harrison, M.L. Phillips, T.M. Nenoff, J. Chem. Soc. Dalton Trans. (2001) 2459.

[13] Y. Wang, J. Yu, Y. Du, Z. Shi, Y. Zou, R. Xu, J. Chem. Soc. Dalton Trans. (2002) 4060.

[14] W.T.A. Harrison, M.L. Phillips, J. Stanchfield, T.M. Nenoff, Inorg. Chem. 40 (2001) 895.

[15] W.J. Dong, G.H. Li, Z. Shi, W.S. Fu, D. Zhang, X.B. Chen, Z.M. Dai, L. Wang, S.H. Feng, Inorg. Chem. Commun. 6 (2003) 776.

[16] W.T.A. Harrison, R.M. Yeates, M.L. Phillips, T.M. Nenoff, Inorg. Chem. 42 (2003) 1493.

[17] D. Whang, N.H. Hur, K. Kim, Inorg. Chem. 34 (1995) 3363.

[18] Y.L. Liu, L.Y. Na, G.S. Zhu, S.H. Feng, W.Q. Pang, R.R. Xu, J. Solid State Chem. 149 (2000) 107.

[19] A.N. Christensen, A. Bareges, R.B. Nielsen, R.G. Hazell, P. Norby, J.C. Hanson, J. Chem. Soc. Dalton Trans. (2001) 1611.

[20] M. Tsuboi, J. Am. Chem. Soc. 79 (1957) 351.

[21] C.J. Pouchent, The Aldrich Library of Infrared Spectra, Aldrich Chemical Co., Inc., Wisconsin, WI, 1970.

[22] J. Chen, R.H. Jones, S. Natarajan, M.B. Hursthouse, J.M. Thomas, Angew. Chem. Int. Engl. 33 (1994) 639.

[23] G. Schäfer, H. Borrmann, R. Knicp, Microporous Mesoporous Mater. 4 (2000) 161.

[24] Software Packages SMART and SAINT, Siemens Analytical X-ray Instruments Inc., Madison, WI, 1996.

[25] G.M. Sheldrick, SHELXTL-NT, Version 5.1, Bruker AXS Inc., Madisom WI, 1997.

[26] D.T. Cromer, J.T. Waber, International Tables for X-ray Crystallography, Vol. 4, Kynoch Press, Birmingham, AL, 1974 (Table 2.2A).

[27] D.J. Williams, J.S. Kruger, A.F. Mcleroy, A.P. Wilkinson, J.N. Hanson, Chem. Mater. 11 (1999) 2241.

[28] H.M. Yuan, J.S. Chen, G.S. Zhu, J.Y. Li, J.H. Yu, G.D. Yang, R.R. Xu, Inorg. Chem. 39 (2000) 1476.

[29] D.T. Cromer, J.B. Mann, Acta Crystallogr. A 24 (1968) 321.

[30] K.O. Kongshaug, H. Fjellvag, K.P. Lillerud, J. Chem. Mater. 9 (1999) 3119.

[31] W.T.A. Harrison, Z. Bircsak, L. Hannooman, J. Solid State Chem. 134 (1997) 148.

[32] S. Oliver, A. Kuperman, G.A. Ozin, Angew. Chem. Int. Ed. 37 (1998) 46.

[33] S. Natarajan, Inorg. Chem. 41 (2002) 5530.

[34] C.N.R. Rao, S. Natarajan, S. Neeraj, J. Am. Chem. Soc. 122 (2000) 2810.

[35] A.M. Chippindale, S. Natarajan, J.M. Thomas, R.H. Jones, J. Solid State Chem. 111 (1994) 18 and the references therein.

[36] S. Natarajan, Chem. Comm. (2002) 780 and the references therein.

[37] K. Burger, Coordination Chemistry: Experimental Methods, Butterworth, London, 1973.

[38] J.R.D. DeBord, R.C. Haushalter, J. Zubieta, J. Solid State Chem. 125 (1996) 270.